

SUPPLEMENTAL FIGURE LEGENDS

Figure S1. Microscopy analysis of melanoma cells, following their transduction with shFZD3.

(A) Representative images of melanoma cell culture densities following transduction of control shRNA (shSC) or shFZD3 into the M727, M525 and M1626 cells. (B) Morphological characteristics of colonies of control shRNA (shSC) or shFZD3 transduced melanoma cells M727, M525 and M1626. Scale bar is set at 200 μm .

Figure S2. FZD3 cDNA overexpression in shFZD3 cells rescues FZD3 mRNA, protein levels and *in vitro* tumorigenic phenotype of melanoma cells.

(A) FZD3 mRNA levels were analyzed by qRT-PCR in the cells expressing either FZD3_FL or pLM plasmids and transduced with shFZD3 lenti-vectors. (B-C) FZD3 protein levels were analyzed using immunofluorescence and FZD3 specific antibody. Y-axis indicates relative FZD3 protein fluorescence intensity (F.I.). Red color indicates positive FZD3 staining. Scale bar is set at 50 μm . Error bars represent SEM of duplicate experiments with three replicates each. * $p < 0.05$, ** $p < 0.005$. (D) Proliferation kinetics of melanoma cells transduced with an indicated plasmids; relative fold change in cell number over time period is plotted. (E) Colony forming capacity of FZD3_FL or pLM M727 cells following control shRNA (shSC) or shFZD3 mediated knockdown. Error bars represent SEM of duplicate experiments with two replicates each *** $p < 0.0005$.

Figure S3. *BRAF*^{V600} mutation hot spot sequence analysis.

Sequence analysis of the *BRAF*^{V600} region in the cells derived from three melanoma patients surgical samples used in the study, M525, M727 and M1626. Nucleotide substitutions are shown in Red and Green mapped against wild type sequence of *BRAF*.

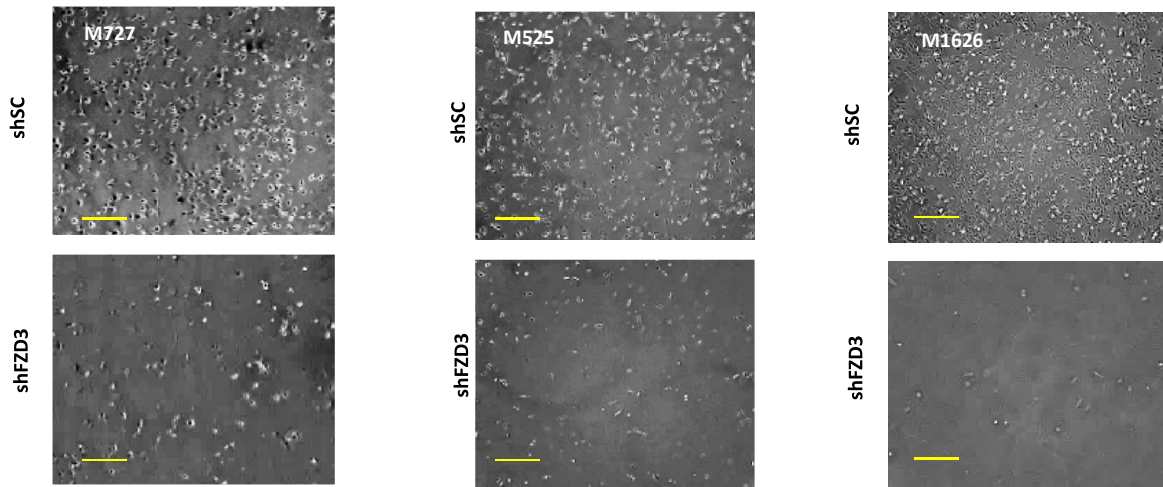
Figure S4. Microscopy analysis of metastases in mouse organs following transplantation of M727 cells.

(A) H&E Kidney tissue section images from representative three mice intradermally xenotransplanted with shSC transduced M727 cells (upper row) or shFZD3 transduced M727 melanoma cells (lower row). (B) H&E Lung tissue section images from representative three mice intradermally xenotransplanted with shSC transduced M727 cells (upper row) or shFZD3 transduced M727 melanoma cells (lower row). Black dotted line outlines metastatic lesions. Scale bar is set at 500 μm .

Figure S5. High levels of FZD3 are associated with melanoma progression and adversely correlate with patient survival.

(A) Relative expression of FZD3 mRNA was analyzed for previously reported melanoma patient cohorts (A) GSE8401 (n=83) and (B) GSE6517 (n=104) who were subdivided into primary and metastatic categories based on associated clinical information. (C) A Kaplan-Meier survival plot of melanoma patients using previously reported cohorts (C) GSE 19234 (n=44) and (D) GSE 65904 (n=130), stratified based on FZD3 mRNA expression level (high expression vs. low). The p value was calculated using the Log-ranked test. (E) Analysis of FZD3 protein expression in melanoma patient tissue arrays.

A



B

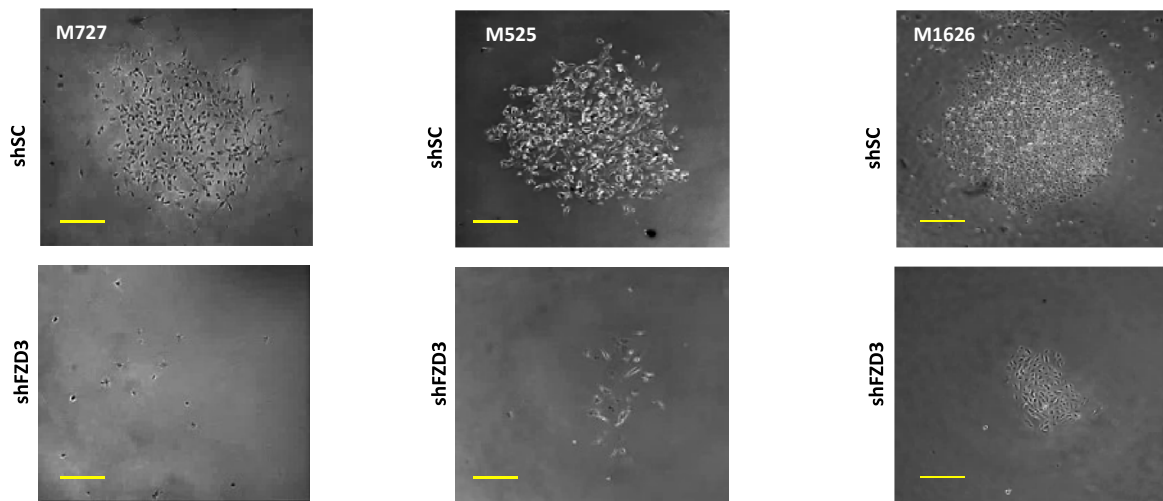


Figure S1.

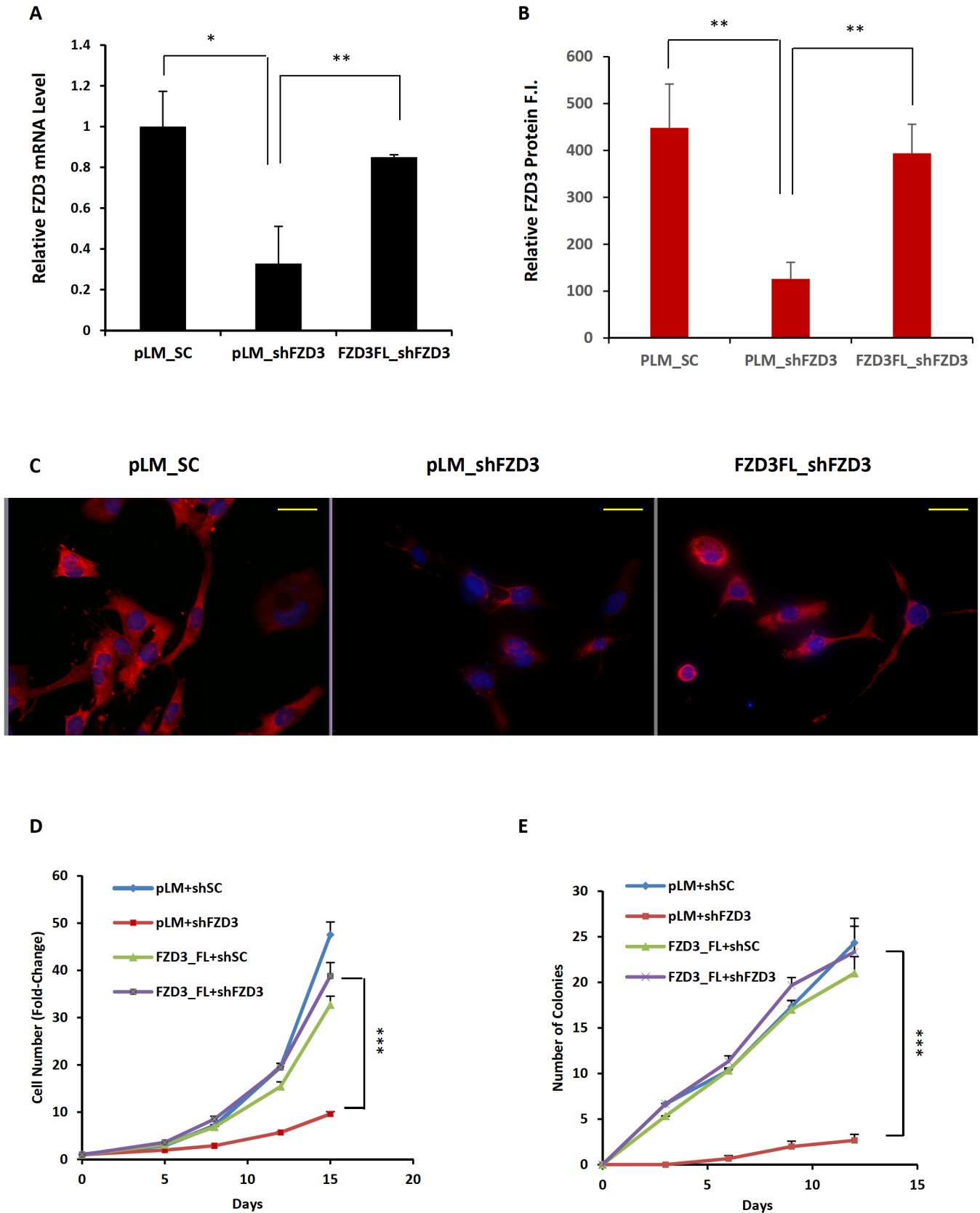


Figure S2.

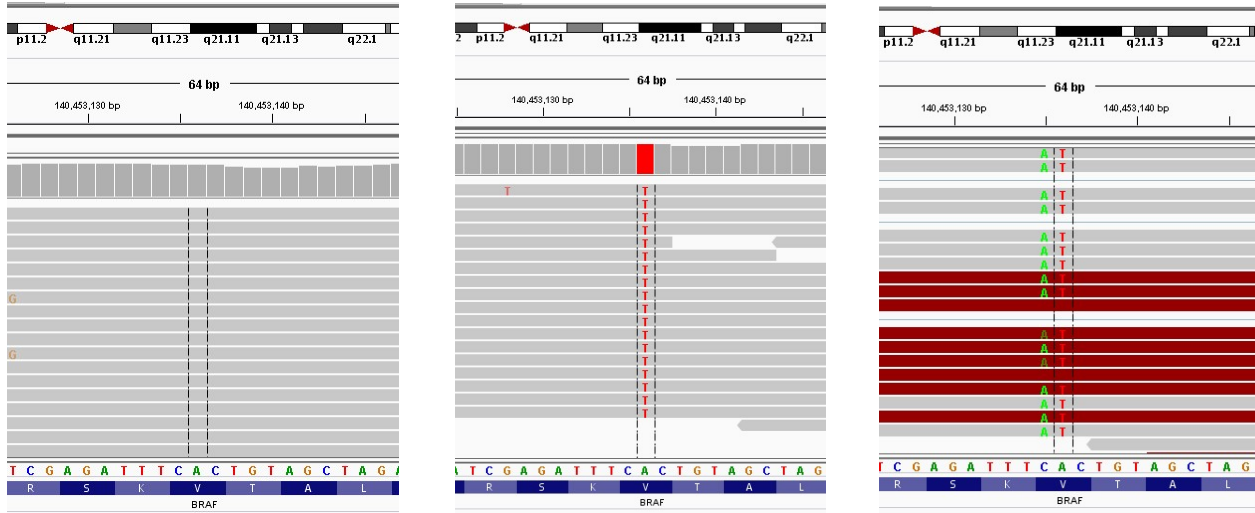
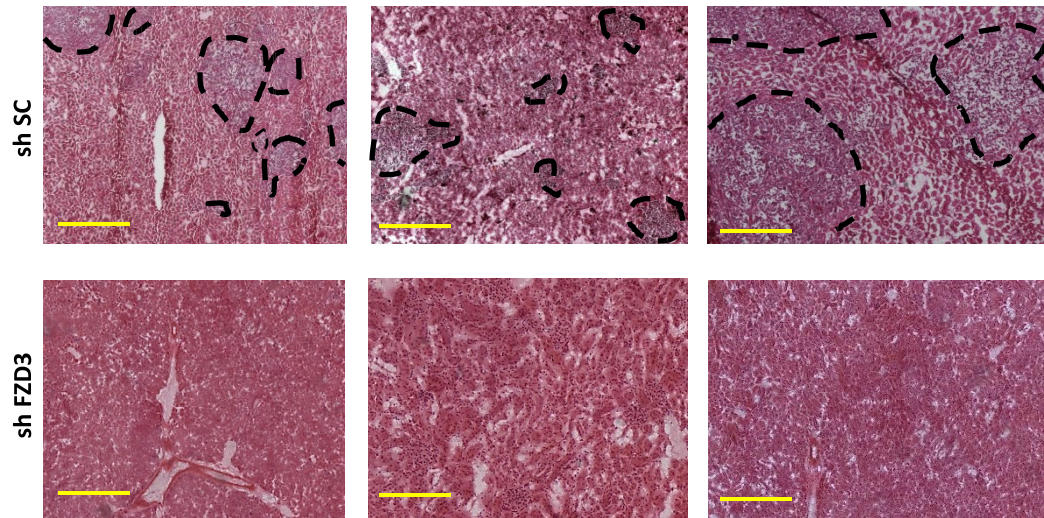


Figure S3.

A

Kidney metastases



B

Lung metastases

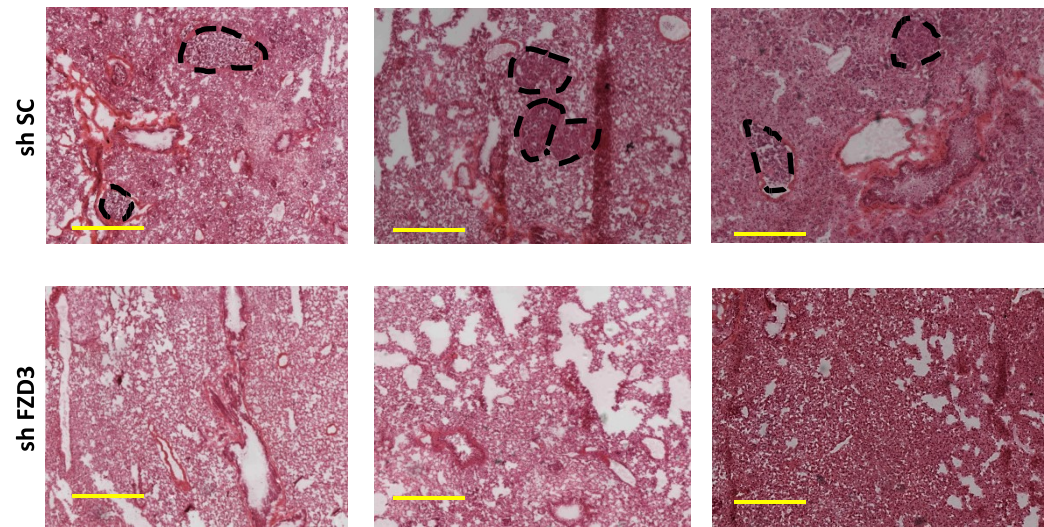


Figure S4.

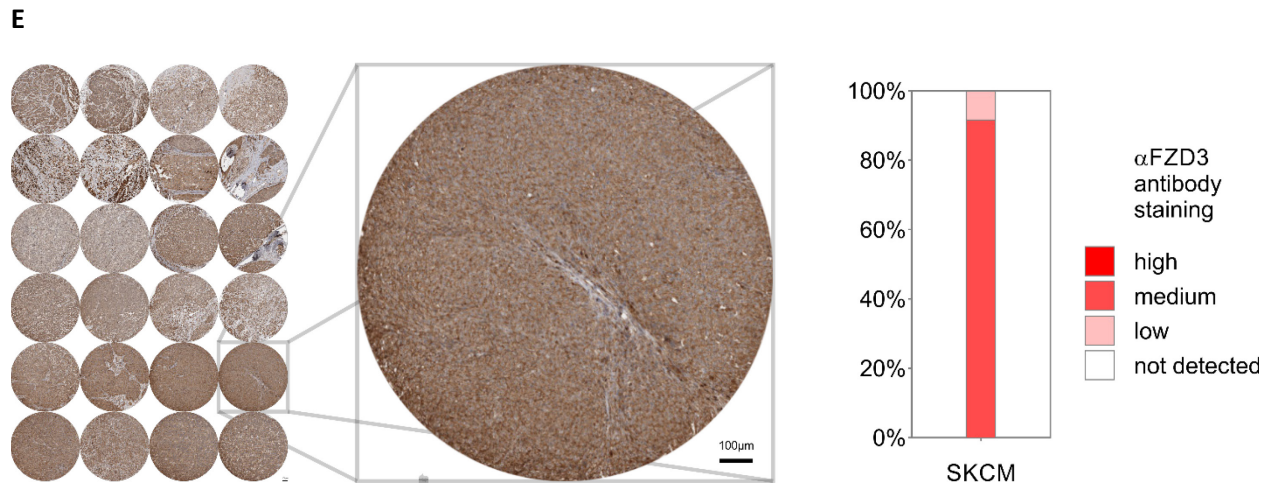
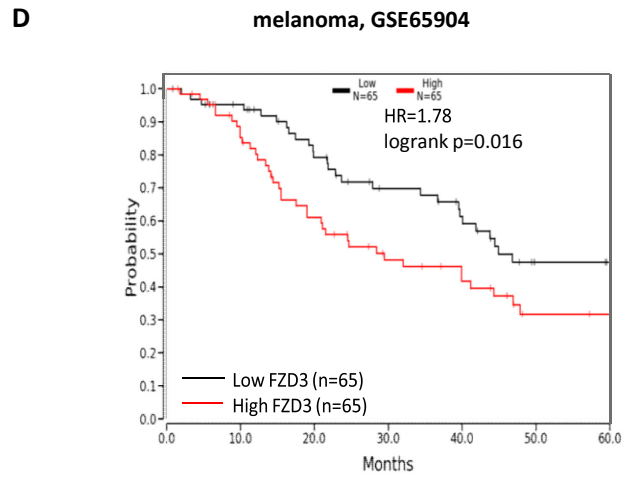
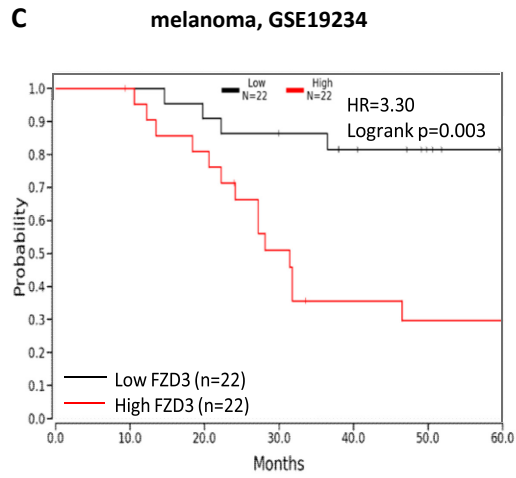
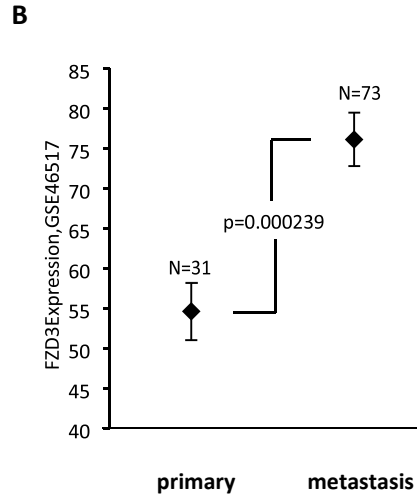
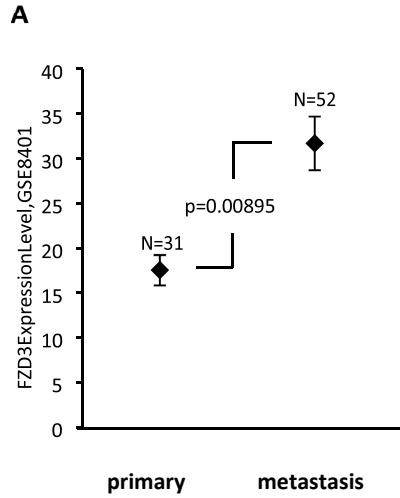


Figure S5.

Table S1. Biological characteristics of patient derived melanoma cell samples.

Melanoma Patient ID	BRAF Status	<i>in vivo</i> properties
M525	<i>BRAF^{WT}</i>	pigmented; slow growing; no metastatic disease in mice
M727	<i>BRAF^{V600E}</i>	unpigmented; highly aggressive; frequently forms metastases in multiple organs of mice
M1626	<i>BRAF^{V600D}</i>	unpigmented; slow growing; no metastatic disease in mice

Table S2. qRT-PCR Oligonucleotides primers used in this study.

Gene target	Forward sequence (5' → 3')	Reverse sequence (3' → 5')
<i>FZD3</i>	ggattggttctcgggatttccg	agtgtgacacgtccatattcca
<i>18S</i>	gcccgaagcgtttactttga	tccattattcctagctgcggt
<i>CCNA2</i>	tgttgggcaactctgcg	ctgccttttccgggttgata
<i>CCNB1</i>	taaggcgaagatcaacatggc	ttttggcctgcagttgttca
<i>CCNB2</i>	caaccagagcagcacaagta	tggtttgacagaagcagtagg
<i>CCND1</i>	ctgcgaagtggaaacctcc	acctccttctgcacacattt
<i>CCNE1</i>	gagcgggacacatgaag	gtcacgtttgccttctctt
<i>CCNE2</i>	gccacctgtattatctgggg	tcaggcaaaggtgaaggatt
<i>CDK1</i>	acaggtcaagtggtagccat	ttgcagtactaggaaccct
<i>CDK2</i>	gtggaaaagatcggagaggg	cggattttcttaagcgccac
<i>CDK4</i>	gaaattggtgtcggtgcccta	ttggggactctcacactctt

SUPPLEMENTAL AND EXTENDED MATERIAL AND METHODS

Cell growth and colony formation assays

Transduced melanoma cells were seeded in a 6-well plate in duplicates and grown at 37°C, 5% CO₂. At indicated days Resazurin reagent (Promega) was added to the cell culture for 30 minutes after which the media was removed and transferred to the black 96-well tissue culture plate for fluorescence readings. Fluorescence and absorbance were subsequently measured using a plate reader (Biotech Synergy HT). Fluorescence values were normalized to the background readings collected from the wells that had no growing cells but contained growth culture media and Resazurin reagent. For adherent colony formation assays, 10³ cells were seeded in 6-well plates and cultured at 37°C, 5% CO₂. Numbers of colonies were counted every 3 days for 2 weeks under light microscope. Cell morphological images were taken by EVOS XL Core Imaging System (Thermo Fisher, CA, USA). At the end of the assay, the plates were washed with PBS, fixed with MeOH and stained with Crystal violet.

In vivo tumor growth assay

Tumor cells were suspended in 35 µL of Matrigel solution, then mixed with 65 µL of 2% HBSS prior to injection. Cells were injected into 2 flanks of the NOD. Cg-Prkdc^{scid} Il2rgtm1Wjl/SzJ (NSG) mice (100 cells per injection, n=10). Tumor related symptoms were monitored every three days within each population. Tumors were measured periodically using external calipers and their size was determined using modified ellipsoid formula ($v = \pi/6 \cdot 1.63\sqrt{(L \times W)^3}$). At the end of the monitoring period mice were euthanized, tumor and internal organs were surgically removed and embedded in Tissue-Plus O.C.T. compounds (Fisher Healthcare, CA). Cyro-sectioning was done at -20°C with Leica CM3050 system (Leica, Germany). Sections were stained with hematoxylin and eosin (H&E). Images were taken by Nikon TI-E fluorescent microscope.

Analysis of cancer patient survival based on FZD3 expression levels

Gene expression and clinical data were analyzed for previously described cohorts of melanoma patients: GSE8401 (n = 83) and GSE46517 (n = 84). Mean FZD3 mRNA expression was analyzed using GEO2R software (<https://www.ncbi.nlm.nih.gov/geo/geo2r/>). Clinical and gene expression data linked to individual patient survival follow up was downloaded and analyzed using KM Plotter. Briefly, patients were stratified into high and low groups based on median FZD3 expression and Kaplan-Meier analysis was performed for overall survival. *p* values were determined using a log-rank test, confidence interval (CI) was set at 95, hazard ratio (HR) was determined using a univariate Cox regression model, values are shown for the relationship of outcomes to dichotomous expression of FZD3.

qRT-PCR

Total RNA was extracted from cancer cells using Trizol reagent (Life Technologies). The mRNAs were reverse transcribed into cDNAs using Verso cDNA synthesis kits (Life Technologies), followed by real-time PCR using KAPA SYBR® FAST qPCR Master Mix (2X) Kit (Sigma-Aldrich, MO, USA). Gene-specific primer sets are summarized in Supplemental Table 2. Values were normalized against 18S using the $\Delta\Delta$ CT method^{1,2}. Data are shown as means and standard deviations (SD) with unpaired Student's t-test with *p* value < 0.05.

Western blot

Cells were lysed with RIPA buffer and protein concentration was determined by BCA assay (Pierce). Protein lysates were separated by SDS-PAGE, transferred to nitrocellulose membranes (Bio-Rad), blocked with 5% milk/TBS, and probed with antibodies in 4°C overnight. The following antibodies were used for Western blot: rabbit anti-GAPDH, (Cell Signaling Technology, Danvers, MA, USA), mouse anti-CDK1, rabbit anti-CDK2, mouse anti-CDK4 (Santa Cruz, Dallas, TX, USA), rabbit anti-cyclin D1, rabbit anti-cyclin E2, rabbit anti-cyclin B1, anti- β -catenin (Cell Signaling Technology, Danvers, MA, USA). All primary antibodies were used at 1:1000 dilution. Membranes were washed three times for 5 min and incubated with a 1:1000 dilution of horseradish peroxidase-conjugated anti-rabbit or anti-mouse (Sigma-Aldrich, MO, USA) antibodies. Blots were washed three times and developed with the ECL system (Pierce) according to the manufacturer's protocols.

Cell immunostaining and analysis

Cells were grown in 4-well Lab-Tek chamber slides and fixed in 4% paraformaldehyde. The slides were incubated with primary antibodies FZD3 (1:200) (MAB1001 R&D system, MN, USA), β -catenin (1:100) (#8480 Cell Signaling), following staining with the secondary antibody Alexa Fluor 594 (1:400) or Alexa Fluor 488 (1:400), (Life technologies, CA). Nuclei were visualized using DAPI reagent. Following immunostaining, immunofluorescent images were taken using a Nikon TI-E fluorescent microscope and a minimum of 10 fields were analyzed for the quantification of positive target protein staining over total DAPI positive cells using ImageJ.

Dual luciferase assay

Target cells were transduced with shFZD3 or shSC lentiviruses, followed by transient transfection of TOPFLASH and FOPFLASH plasmids (2 μ g) (Addgene) with renilla luciferase plasmid (0.5 μ g) using ViaFect Transfection reagent (Promega, Madison, WI, USA). 3 days after infection and transfection, cells were counted and lysed in passive luciferase lysis buffer (Promega). Luciferase assay was performed with the Dual Luciferase Reporter assay system (Promega). Luminescence was measured using Sirius Luminometer V3.2. Renilla luciferase reporter was used to normalize for transfection efficiency.

1. Schmittgen TD, Livak KJ. Analyzing real-time PCR data by the comparative C(T) method. *Nat Protoc.* 2008;3(6):1101-8.
2. Singh SJ, Turner W, Glaser DE, McCloskey KE, Filipp FV. Metabolic shift in density-dependent stem cell differentiation. *Cell Commun Signal.* 2017 Oct 20;15(1):44. doi: 10.1186/s12964-017-0173-2.